23rd ABCM International Congress of Mechanical Engineering
December 6-11, 2015, Rio de Janeiro, RJ, Brazil

ENERGY HARVESTING SYSTEM PARAMETERS BEHAVIOR FOR ACTIVE CONTROL

Douglas da Costa Ferreira
UNESP - Univ. Estadual Paulista, Postdoctoral, Ilha Solteira/SP, Brazil
dcferreira@ufmt.br

Fábio Roberto Chavarette
UNESP - Univ. Estadual Paulista, Ilha Solteira/SP, Brazil
fabioch@mat.feis.unesp.br

Nelson José Peruzzi
UNESP - Univ. Estadual Paulista, Jaboticabal/SP, Brazil
peruzzi@fcav.unesp.br

Jean-Marc Stephane Lafay
Federal Technological University of Paraná, Pato Branco/PR, Brazil
jeanmarc@utfpr.edu.br

Ana Paula Quadros de Oliveira
Federal University of Mato Grosso, Rondonópolis,/MT, Brazil
aquadros.oliveira@gmail.com

Danielle da Silva Rocha
Federal University of Mato Grosso, Rondonópolis,/MT, Brazil
danielle.r2@hotmail.com

Vinícius Favretto
Federal University of Mato Grosso, Rondonópolis,/MT, Brazil
vinicius_favreto@hotmail.com

Anne Karoline Pires Oliveira
Federal University of Mato Grosso, Rondonópolis,/MT, Brazil
karol.engmec@gmail.com

Vanessa Cruz Oliveira
Federal University of Mato Grosso, Rondonópolis,/MT, Brazil
nessaoliveira56@gmail.com

Abstract. *A numeric simulation of an energy harvesting system based in vibration and subject to a periodic excitation presented the amount output voltage according to system parameters. It was projected a Linear Matrix Inequalities (LMI) controller to change system parameters as relativity damping and rigidity. It was possible to observe that excitation variation of relativity parameters outcomes in a singular behavior describing the controller actuation for mechanical energy transfer maximization. The research is part of PhD thesis related to energy harvesting system enhancement in a deep discussion about mechanical energy transfer related to parameters behavior*.

Keywords: *energy harvesting systems, linear matrix inequalities, parameters behavior, efficiency*

1. INTRODUCTION

Energy harvesters are those systems that convert some of small scale energy to electric energy (Chen et al., 2010). The means to process that transformation variety from small gradients of heat to microwave radio frequency (Thomas et al., 2006). One of promised source of energy to be converted via energy harvesting systems is environment vibration (Miller et al., 2011). There are many works published in the past decade concerning energy harvesting and mostly are focusing in enhance their efficiency (Wang and Inman, 2012; Diyana et al., 2012; Noh and Yoon, 2012; Tang et al., 2013; Zhu et al., 2010; Masuda and Senda, 2011). Among the works dealing to piezoelectric energy harvesting the most of them uses the resonance effect as the mean source of vibration to improve efficiency (Roundy et al., 2003; Stoppel et al., 2011; Baù et al., 2011; Kim et al., 2012). The harness of resonance is because the ambient vibration has a large frequency bandwidth and the resonance occurs only for a narrow band and the projects presented are efficient only for this small range (Harne and Wang, 2013; Tang et al., 2013; Jung et al., 2013).

Another solution is to utilize a controller to driven the energy harvesting system to a maximum interaction between the vibration source and the vibrational system resulting in a maximum energy transduction (Wu et al., 2006; Eichhorn et al., 2009; Peters et al., 2009; Zhu et al., 2010). A prior work was developed by Ferreira et al. (2014) using a Linear Matrix Inequalities controller for a harmonic excitation to a well-defined piezoelectric energy harvesting system of Erturk and Inman (2011). As a research result there was a significant increase of net output power from controlled system compared to the open loop system.

To understand the system behavior it is possible to analyze the amount of change of system parameters according the controller output signal and compare this change to the amount of energy increased to transduction process. In this way it is possible to conclude how much parameter changes are influencing to the efficiency gain and then could be possible to improve future researches by focusing in singular parameters adjustment.

2. ENERGY HARVESTING MODEL

A proposed bimorph energy harvesting cantilever excited by an exogenous source and coupled to a circuit load (Erturk and Inman, 2011) is given in Figure 1. In this design a cantilever with two layers of piezoelectric material (PZT) is modeled dimensionless according resonance where ζ is damping factor, χ is piezoelectric mechanical coupling coefficient, Λ is reciprocal of time constant and κ is piezoelectric electric coupling coefficient. The system variables are x for tip beam position and v for system output voltage load. The red arrows indicate the electrical direction and the electricity follow from the PZT layers to output voltage in piezoelectric direct effect.

The excitation parameters is collected from output voltage reading as input signal and a portion of the output voltage returns to PZT layers passing by a control processor to driven the system behavior to maximum interaction to exogenous excitation in piezoelectric indirect effect. This portion of voltage that returns to PZT layers are the feedback control signal and will increase energy harvesting system efficiency since the percentage of resulting kinetic energy to be converted in output voltage was greater than the energy used to control the system behavior.

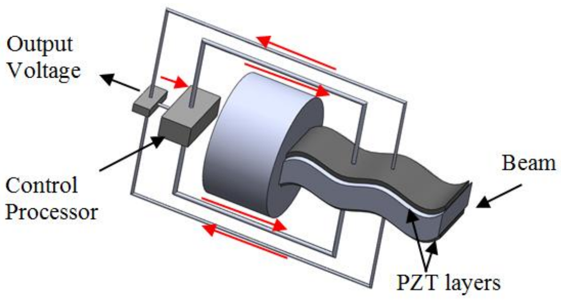

Figure 1. Bimorph cantilever

Considering the case of exogenous excitation being a periodic (harmonic) excitation the mathematical system model is presented according Erturk and Inman (2011), given by:

$$\begin{aligned} &\ddot{x} + 2\zeta\dot{x} + \tfrac{1}{2}x - \chi v = f\cos\Omega t \\ &\dot{v} + \Lambda v + \kappa\dot{x} = 0 \end{aligned} \tag{1}$$

were f is dimensionless acceleration force and Ω is dimensionless excitation frequency. Isolating $\ddot{x}$ and $\dot{v}$ in equation (1),

$$\begin{aligned} &\ddot{x} = -\tfrac{1}{2}x - 2\zeta\dot{x} + \chi v + f\cos\Omega t \\ &\dot{v} = -\kappa\dot{x} - \Lambda v \end{aligned} \tag{2}$$

and Adopting $y_1 = x$, $y_2 = \dot{x}$ and $y_3 = v$, the equation is given as

$$\begin{aligned} &\dot{y}_1 = y_2 \\ &\dot{y}_2 = -\frac{1}{2}y_1 - 2\zeta y_2 + \chi y_3 + f\cos\Omega t \\ &\dot{y}_3 = -\kappa y_2 - \Lambda y_3 \end{aligned} \tag{3}$$

Parameters for the model are determined numerically and experimentally tested according Erturk and Inman (2011) and are $\zeta = 0.01$, $\chi = 0.05$, $\Lambda = 0.05$, $\kappa = 0.5$, $f = 0.083$ and $\Omega = 0.8$. The system behavior is determined by performing Runge-Kutta fourth order method for solving ordinary differential equations for given parameters to the space-state form. The numerical simulation considered initial conditions $x(0) = 1$, $\dot{x}(0) = 0$ and $v(0) = 0$ and time samples from 0 to 2,500 in interval of 0.1 totalizing 25,000 samples in Figures 2a and 2b and samples from 2,000 to 2,500 in interval of 0.1 totalizing 5,000 samples in Figure 2c to exclude transient behavior.

a)

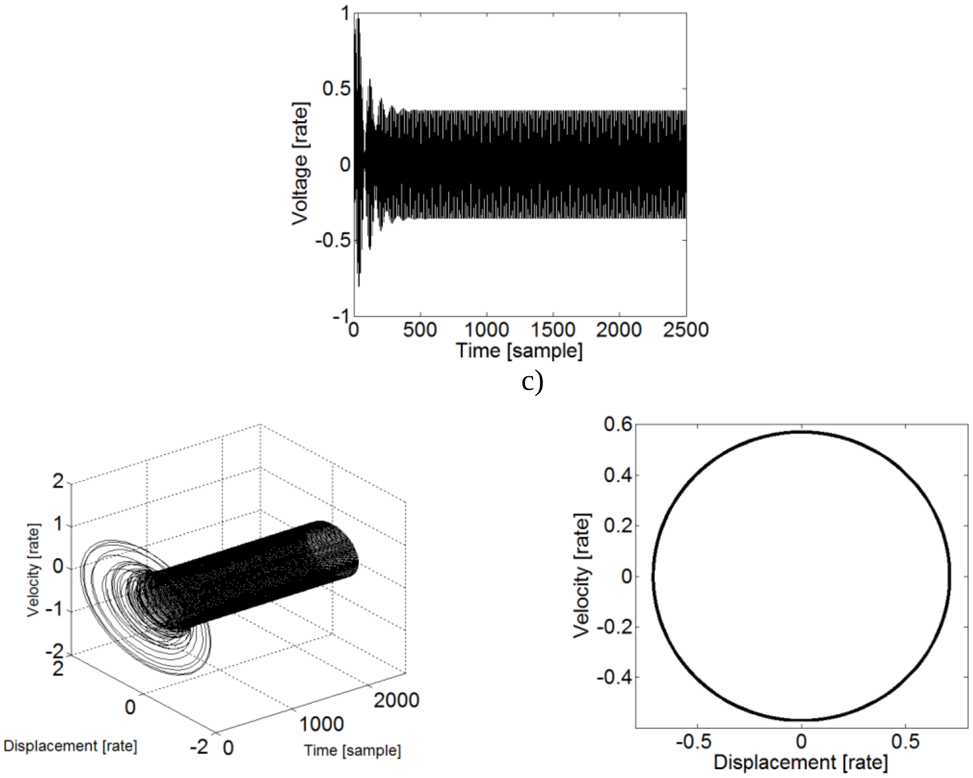

Figure 2. (a) voltage rate, (b) time history, (c) phase portrait.

For given parameters the system eigenvalues are shown in Table 1 and since all eigenvalues do have real part negative the system can be considered stable.

Table 1. Eigenvalues

λ_1	-0.0112 + 0.7244i
λ_2	-0.0112 - 0.7244i
λ_3	-0.0476 + 0.0000i

3. CONTROLER DEFINITION

To ensure maximum energy harvested it was coupled a controller using Linear Matrix Inequalities (LMI) according Optimum Control H∞. An LMI Control Driven utilizes feedback state to optimize the interaction between exogenous excitation w and result signal y (Antwerp and Braatz, 2000). A sufficient condition for LMI control driven is the existence of a matrix $X = X' > 0 \in \mathcal{R}^{nxn}$ and $Y \in \mathcal{R}^{mxn}$. The parameter μ refers to the objective function and to enhance energy harvesting system the function must be maximized.

$$\begin{cases} \max \mu \\ \begin{bmatrix} AX + XA' - B_2Y - Y'B_2' & XC' + Y'D' & B_1 \\ CX + DY & -I & 0 \\ B_1' & 0 & -\mu I \end{bmatrix} < 0 \\ X > 0 \end{cases} \tag{4}$$

The space-state model (Chadli et al., 2013) for the proposed system is given as

$$\begin{cases} \dot{x} = Ax + B_1 w + B_2 u \\ y = Cx \end{cases} \tag{5}$$

were A is state matrix, B_1 is the excitation vector, B_2 is the control vector and C is the vector of system result. The relation between matrices is explained in the block diagram presented in Figure 7.

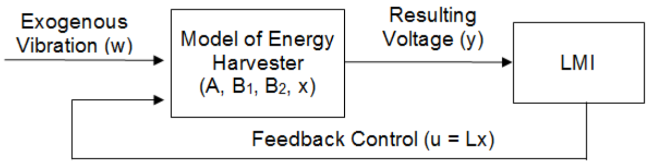

Figure 3. Block diagram of the controlled systems.

4. PARAMETERS BEHAVIOR

The dynamical model showed in equation (2) can be rewritten in matrix form as

$$\begin{Bmatrix} \dot{x}_1 \\ \dot{x}_2 \\ \dot{x}_3 \end{Bmatrix} = \begin{bmatrix} 0 & 1 & 0 \\ -\frac{1}{2} & -2\zeta & \chi \\ 0 & -\kappa & -\Lambda \end{bmatrix} \begin{Bmatrix} x_1 \\ x_2 \\ x_3 \end{Bmatrix} + \begin{bmatrix} 0 \\ 1 \\ 0 \end{bmatrix} f \cos \Omega t \tag{6}$$

The LMI matrices are resulting from replacing given parameters for linear model in matrix form, and are

$$A = \begin{bmatrix} 0 & 1 & 0 \\ -0.5 & -0.02 & 0.05 \\ 0 & -0.5 & -0.05 \end{bmatrix},$$

$$B_1 = \begin{bmatrix} 0 \\ 0.083 \cos \Omega t \\ 0 \end{bmatrix},$$

$$B_2 = \begin{bmatrix} 1 \\ 1 \\ 1 \end{bmatrix} \; e \; C = \begin{bmatrix} 1 & 0 & 0 \end{bmatrix} \tag{7}$$

The system actual state is given for the parameters of state matrix A and de control signal is the feedback state matrix (A_f) as shown

$$A_f = A - B_2 L \tag{8}$$

To accomplish a control simulation the regulator parameter is the dimensionless frequency Ω which is ranging from 0.4 to 1.0. For a dimensionless frequency $\Omega = 0.4$ the excitation vector is

$$B_{1\_0.4} = \begin{bmatrix} 0 \\ 0.083 \cos 0.4t \\ 0 \end{bmatrix} \tag{9}$$

Replacing A, $B_{1\_0.4}$, B_2 and C in LMI and solving the inequalities the feedback state vector is $L_{0.4} = [\,0.0194 \quad 0.4894 \quad -0.1587]$. The feedback state matrix is derived from A, B_2 and $L_{0.4}$ and resulting in the feedback parameters $\zeta = 0.2547$, $\chi = 0.2087$, $\Lambda = 0.0001$ and $\kappa = 0.9894$. Substituting open loop parameter given in Linear model and the feedback parameters for $\Omega = 0.4$ and performing Runge-Kutta fourth order method for solving ordinary differential equations for initial conditions $x(0) = 1$, $\dot{x}(0) = 0$ and $v(0) = 0$ and dimensionless acceleration force $f = 0.083$ the comparison from open loop to controlled system is given in Figure 3. The RMS output voltage from open loop system is 0.0805 and for the controlled system is 4.2202 which gives a gain of 50.84 times.

a)

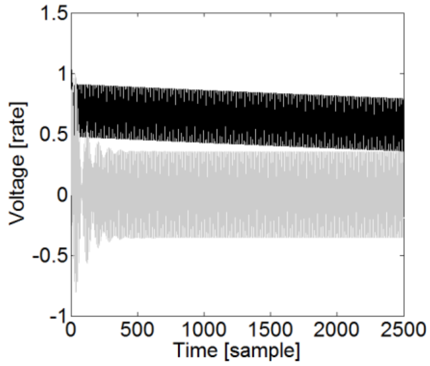

b)

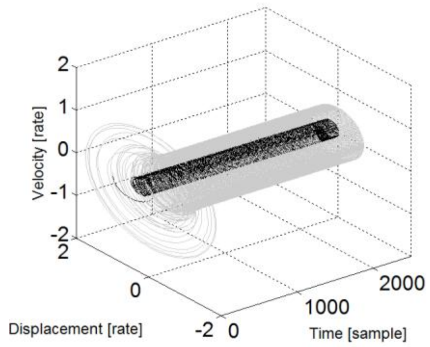

c)

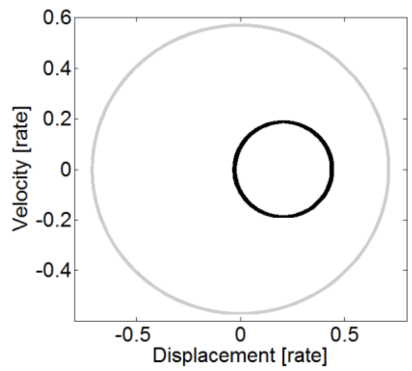

Figure 3. Open Loop (gray line), Controlled (black line). (a) voltage rate, (b) time history, (c) phase portrait.

Applying the same procedure to the other frequencies the controlled parameters are given in Table 1.

Table 1. Parameters and RMS output voltage for Ω = 0.4 to Ω = 1.0.

	Frequency Rate						
Controlled Parameters	0.4	0.5	0.6	0.7	0.8	0.9	1.0
ζ	0.257	0.2491	0.242	0.2324	0.2206	0.2066	0.1892
χ	0.2087	0.2027	0.1956	0.1863	0.1757	0.1637	0.1501
κ	0.9894	0.9783	0.964	0.994	0.9213	0.8932	0.8585
Λ	1.00E-04	1.00E-04	1.00E-04	1.00E-04	1.00E-04	1.00E-04	1.00E-04
RMS Open Loop	0.0805	0.1238	0.3043	5.3812	0.6570	0.1409	0.0756
RMS Controlled	4,2272	4,2505	4,2763	4,3001	4,2676	4,1293	3,9368

The comparison of output energy from open loop to controlled system is given in Figure 4.

a) Ω = 0.4

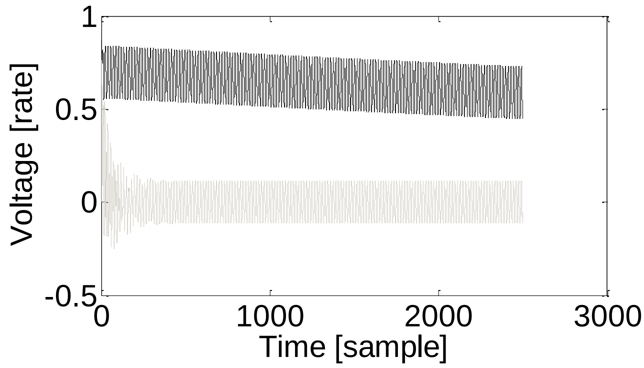

c) Ω = 0.5

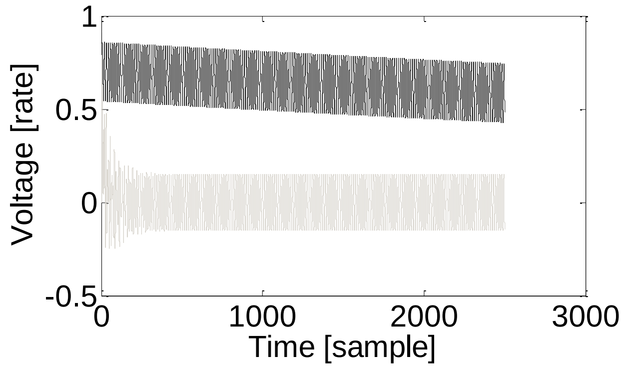

c) Ω = 0.6

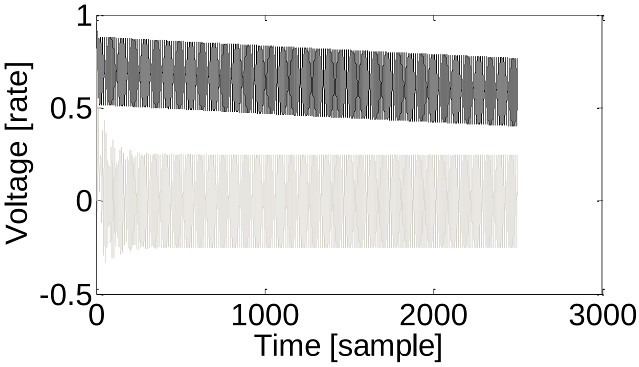

d) Ω = 0.7

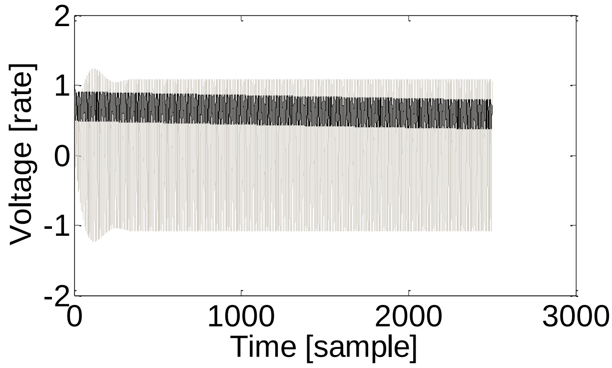

d) Ω = 0.8

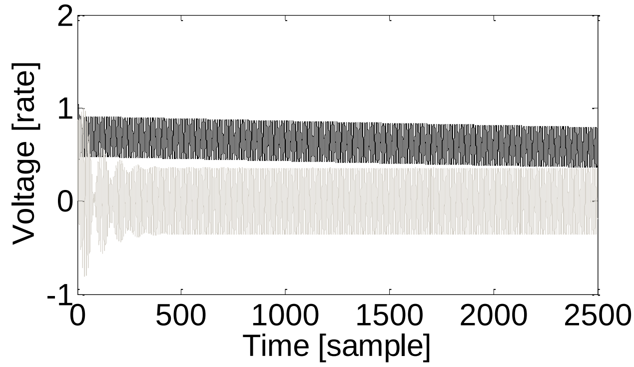

e) Ω = 0.9

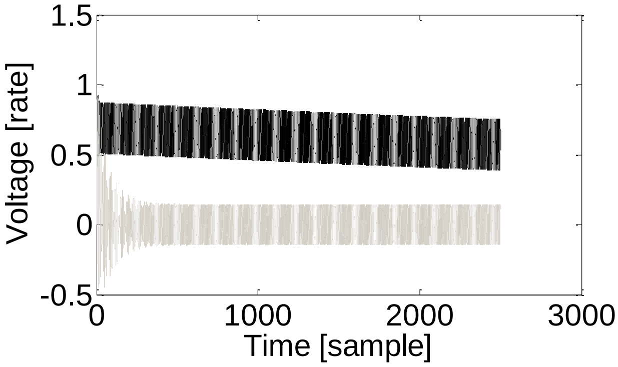

g) Ω = 1.0

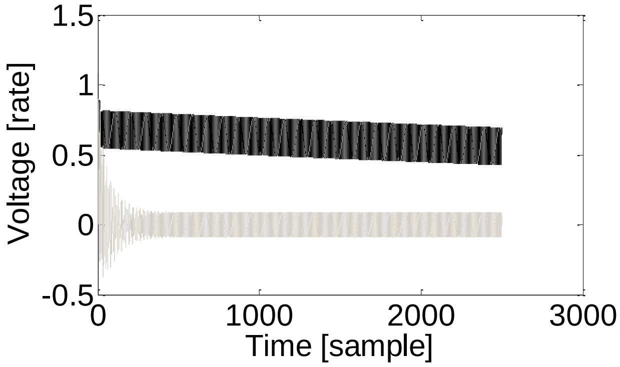

Figure 4. Output voltage. Open Loop (gray line), Controlled (black line).

The consideration of the amount of change of parameters related to the amount of change of RMS output voltage is given in Table 2. It is suppressed the value of Λ because it is close to zero.

Table 2. Amount of change of parameters and RMS output voltage.

	Amount of variation						
Controlled Parameters	0.4	0.5	0.6	0.7	0.8	0.9	1.0
ζ	96,1%	96,0%	95,9%	95,7%	95,5%	95,2%	94,7%
χ	76,0%	75,3%	74,4%	73,2%	71,5%	69,5%	66,7%
κ	49,5%	48,9%	48,1%	49,7%	45,7%	44,0%	41,8%
RMS	98,1%	97,1%	92,9%	-25,1%	84,6%	96,6%	98,1%

It is possible to verify a regular variation from parameters and the RMS output voltage. There were no a significant change of parameters related to RMS variation excluding the resonant effect that is normally explained according physics expected behavior.

5. CONCLUSION

The evaluation of amount of change of controlled parameters via Linear Matrix Inequalities applied to an energy harvesting system based in active piezoelectric effect shows that there were regular variations from parameters amount of change compared to the amount of change of RMS output power. Since the frequency rate do not influence significantly in the amount of change of controlled parameters it is possible to conclude that the principal influence in the RMS output is the energy harvesting system design and the application of active control has a regular increase of system efficiency.

6. ACKNOWLEDGEMENTS

The authors would like to thanks to Federal University of Mato Grosso. Federal Technological University of Paraná. UNESP - Univ. Estadual Paulista, Postdoctoral in Mechanical Engineering program for support. To Fundação de Amparo a Pesquisa do Estado de São Paulo (FAPESP Process No. 2014/16807-3) and Conselho Nacional de Desenvolvimento Científico e Tecnológico (CNPq Process No. 301769/2012-5) for funding. To Fundação Araucária. CAPES. FINEP. Fundação de Amparo a Pesquisa do Estado de Mato Grosso (FAPEMAT) and SETI for scholarship and funding.

7. REFERENCES

Baù, M.; Ferrari, M.; Tonoli, E.; Ferrari, V. *Sensors and energy harvesters based on piezoelectric thick films*. Procedia Engineering, v. 25, p. 737-744, 2011.

Chen, M.; Han, Z. *Controlling and synchronizing chaotic Genesio system via nonlinear feedback control*. Chaos, Solitons and Fractals, v. 17, p. 709-716, 2003.

Diyana, N. H.; Muthalif, A. G. A.; Fakhzan, M. N.; Nordin, A. N. Vibration energy harvesting using single and comb-shaped piezoelectric beam structures: Modeling and simulation. Procedia Engineering, v. 41, p. 1228-1234, 2012.

Eichhorn. C.. Goldschmidtboeing. F.. Porro. Y.. Woias. P. A. *Piezoelectric Harvester with an Integrated Frequency-tuning Mechanism*. PowerMEMS. p. 45-48. 2009.

Erturk. A.. Inman. D. J. *Broadband piezoelectric power generation on high-energy orbits of the bistable duffing oscillator with electromechanical coupling*. Journal of Sound and Vibration. v. 330. n. 10. p. 2339-2353. 2011.

Ferreira. D. C.. Chavarette. F. R.. Peruzzi. N. J. *Optimal Linear Control Driven for Piezoelectric Non-Linear Energy Harvesting on Non-Ideal Excitation Sourced*. Advanced Materials Research. Vols. 971-973. pp 1107-1112. 2014.

Kim, S.-G.; Priya, S.; Kanno, I. Piezoelectric *MEMS for energy harvesting*. Materials Research Society, n. 37, p. 1039-1050, 2012.

Jung, H.-J.; Kim, I.-H.; Min, D.; Sim, S.-H.; Koo, J.-H. *A hybrid electromagnetic energy harvesting device for low frequency vibration*. Proc. of SPIE, v. 8688 , p. 1-4, 2013.

Harne. R. L.. Wang. K. W. *A review of the recent research on vibration energy harvesting via bistable systems*. Smart Mater. Struct.. v. 22. p. 1-12. 2013.

Masuda A.; Senda, A. *A vibration energy harvester using a nonlinear oscillator with self-excitation capability*. Active and Passive Smart Structures and Integrated Systems, v. 7977, p. 1-9, 2011.

Miller. L. M.. Halvorsen. E.. Dong. T.. Wright. P. K. *Modeling and experimental verification of low-frequency MEMS Energy Harvester from ambient vibrations*. Journal of Micromechanics and Microengineering. v. 21. p. 1-13. 2011.

Noh, J. Y.; Yoon, G. H. *Topology optimization of piezoelectric energy harvesting devices considering static and harmonic dynamic loads*. Advances in Engineering Software, v. 53, p. 45-60, 2012.

Peters, C.; Maurath, D.; Schock, W.; Mezger, F.; Manoli, Y. *A closed-loop wide-range tunable mechanical resonator for energy harvesting systems*. J. Micromech Microeng, v. 19, p. 1-9, 2009.

Roundy, S.; Wright, P. K.; Rabaey, J. *A study of low level vibrations as a power source for wireless sensor nodes*. Computer Communications, v. 26, p. 1131-1144, 2003.

Stoppel, F.; Schrödera, C.; Sengera, F.; Wagnera, B.; Beneckea, W. *AlN-based piezoelectric micropower generator for low ambient vibration energy harvesting*. Procedia Engineering, v. 25, p. 721-724, 2011.

Tang. L.. Yaowen. Y.. Soh. C. K. Broadband vibration energy harvesting techniques. *Advances in Energy Harvesting Methods (Chapter Two)*. New York : Springer Science & Business Media. 46p. 2013.

Thomas. J. P.. Qidwai. M. A.. Kellogg. J. C. *Energy scavenging for small-scale unmanned systems*. Journal of Power Sources. v. 159. p. 1494-1509. 2006.

Wang, Y.; Inman, J. D. *A survey of control strategies for simultaneous vibration suppression and energy harvesting via piezoceramics*. Journal of Intelligent Material Systems and Structures, v. 23, n. 18, p. 2021-2037, 2012.

Wu. W.-J.. Chen. Y.-Y.. Lee. B.-S.. He. J.-J.. Peng. Y.-T. *Tunable resonant frequency power harvesting devices*. Smart Structures and Materials. Proc. of SPIE. v. 6169. n. 1. p. 1-8. 2006.

Zhu, D.; Tudor, M. J.; Beeby, S. P. *Strategies for increasing the operating frequency range of vibration energy harvesters: a review*. Meas. Sci. Technol., v. 21, p. 1-29, 2010.

8. RESPONSIBILITY NOTICE

The authors are the only responsible for the printed material included in this paper.